Theoretical Study of Glass Systems Using ab Initio Molecular Electronic Structure Theory. 1. Lithium Metaphosphate Glass

Emmanuel D. Simandiras* and Dimitrios G. Liakos

Theoretical and Physical Chemistry Institute, National Hellenic Research Foundation, 48 Vas. Constantinou Ave., 116 35 Athens, Greece

Received: June 26, 2003; In Final Form: February 6, 2004

A methodology for the theoretical study of glass systems using ab initio molecular electronic structure theory is discussed. Lithium metaphosphate glass of the formula $Li_2O{\cdot}P_2O_5$ is considered, and the choice of models and methods is discussed. The presence and significance of multiple minima on the potential energy surface is also discussed. Four lowest energy structures for the model $(Li_2O{\cdot}P_2O_5)_4$ are given, and vibrational spectra are predicted and compared to experimental data. A structure that would indicate preference for the formation of P−O−P chains in the lithium metaphosphate glass is found to be the most stable energetically in the model. Good overall agreement with experimental infrared and Raman spectra is achieved.

Introduction

The experimental study of noncrystalline solid materials is a subject of great interest to the scientific community, and entire journals are devoted to the reporting of results from such studies. The theoretical studies performed on these materials have been extensive in the areas of molecular dynamics and simulation (see, for example, ref 1 for a good molecular dynamics study of lithium phosphate glasses). On the other hand, research using an ab initio molecular electronic structure theory basis has received less attention. One possible reason for this situation is the difficulty in modeling an amorphous solid system using ab initio computational quantum chemical methods. Although a crystalline solid can be approached by various models that use the periodicity of the infinite system, this same methodology cannot be applied to the theoretical study of a glass material. Previous studies have used small clusters of atoms and ions to model glasses.[2,3] When the size of the cluster model is relatively small, the conclusions that can be drawn regarding the macroscopic properties of the material are limited. When the size of the cluster is increased, the computational difficulty will increase rapidly, but more meaningful results can be obtained for the solid.

In this work we approach the ab initio molecular electronic structure theory study of a glass using a cluster model of a size large enough to have some resemblance to the microscopic regions of the real solid, but also small enough to be tractable by modern ab initio methods. This approach has been used previously by Uchino and Yoko[4] with very encouraging results. Here, we extend this methodology by recognizing that a cluster of, for example, 40 atoms will have *multiple minima* on its potential energy surface, probably lying relatively close in energy. We therefore use a combination of semiempirical and ab initio methods to map these points of interest and try to analyze the structural and spectroscopic properties of a glass using calculations performed at these minima.

The material under study here is the lithium phosphate glass $xLi_2O{\cdot}(1 - x)P_2O_5$, in particular for the case where $x = 1$ (metaphosphate). In pure vitreous P_2O_5 the basic structural unit is the PO_4 tetrahedron, where only three of the four corners are shared, i.e., $POO_{3/2}$, the three bridging oxygen atoms per unit helping the formation of a random three-dimensional structure.[5] When an alkali metal oxide such as Li_2O is added, breakage of some of the P−O−P bonds occurs giving an increasing number of metaphosphate $[PO_2O_{2/2}]^-$ units. This will lead to the presence of long chains and rings in the structure.[6] In the material studied here, where Li_2O and P_2O_5 exist in equal molar quantities, we expect an increased tendency for the formation of metaphosphate structures, hence chains and rings, but also expect to find phosphate ($POO_{3/2}$) and pyrophosphate ($PO_3O_{1/2}{}^{2-}$) units.

A theoretical analysis of an alkali phosphate glass is of interest for many reasons; first, as stated above, the properties of the resulting material will depend on the number and distribution of phosphorus atoms connected by three, two, or one oxygen atoms, and optimized structures from theory can easily provide this information. Second, the vibrational spectra can be predicted and compared to experimental data, where they can be used to aid the interpretation of the measured data. Finally, the atomic numbers of the constituents P, O, and Li in the system are small enough, allowing an extended study using ab initio methods, relatively large cluster models, and reasonable basis sets, to test the feasibility of meaningful ab initio prediction of properties of glass materials.

Models and Methods

To model the $Li_2O{\cdot}P_2O_5$ glass, we choose a cluster model comprising four Li_2O molecules and four P_2O_5 molecules; this totals 40 atoms. In a previous work[4] the structure of the model was predetermined and constrained to be ringlike, in an attempt to force reasonable coordination numbers for as many of the constituents as possible. This led to reasonable agreement with experiment. Here we do not wish to put any constraint on the relative positioning of the lithium and phosphorus oxide molecules in space, and expect to draw further conclusions on the relative positioning of the atoms in the model, driven by the requirement of energy minimization alone. To approach from various angles the potential energy surface (PES), and find all if possible of the lowest lying energy minima, we propose in this work the following strategy: we position the eight (four lithium oxide and four phosphorus oxide) molecules or in some cases the equivalent atoms comprising the model in three

10.1021/jp035819o CCC: $27.50
Published on Web 04/01/2004

dimensions using a combination of chemical intuition and randomness. Then, using a fast semiempirical method such as AM1[7] or PM/3,[8,9] we optimize this structure. From as many possible random or intuitively chosen starting positions, we produce a number of different minima obtained at the semiempirical level; the six to eight lowest lying of these are then optimized using the Hartree−Fock self-consistent field (HF SCF) method using a reasonably sized basis set with one set of polarization functions, namely the 3-21G*.[10,11] A number of minima on the PES at the HF/3-21G* are thus obtained; this is not necessarily the same number as the semiempirical minima, as some of the latter may have converged to the same HF/3-21G* minimum, or some may not have converged at all. The HF/3-21G* minima are confirmed by calculating the energy second derivatives requiring that six "zero" frequencies exist and are ordered in ascending energy.

In this study we have performed semiempirical optimizations from at least 30 different initial positionings of the eight Li_2O and P_2O_5 molecules. From these, 12 minima obtained at the PM/3 level of theory were resubmitted to the HF/3-21G* energy optimization procedure, giving eight distinct energy minima.

All calculations, semiempirical and ab initio, were performed using the GAUSSIAN 98[12] suite of programs, and visualization was done using the GAUSSVIEW package.

Results and Discussion

1. Structures. The methodology described in the previous section yielded a number of HF/3-21G* level minima on the potential energy surface of the $(Li_2O{\cdot}P_2O_5)_4$ system; of these, the four lowest lying in energy, structures I−IV, are given in this section. It is useful to note at this stage that there is no *guarantee* that structure I is the *global* minimum of the PES, but the extensive mapping and optimization of numerous structures suggest that this is the case.

Views of structures I−IV are given in Figure 1i−iv. The total energies and average bond lengths are given in Table 1, but full geometrical data are available from the authors upon request.

An almost uniform variation of the average phosphorus to bridging oxygen ($P-O_b$) and phosphorus to nonbridging oxygen ($P-O_{nb}$) bond lengths is noted in Table 1 for the four structures. In all cases a difference of about 0.1 Å, the average $P-O_b$ being longer, is consistent with previous theoretical studies and experimental finds (see refs 1 and 4 and references therein).

Structure I (Figure 1i) shows two Li-bridged P−O−P rings on each end of the overall D_{2h} structure. This is compatible with the formation of P−O−P chains, as has been proposed earlier for alkali metaphosphate glasses,[13] these chains closing into eight-membered rings due to the finiteness of the model and the necessity for energetic stabilization. The two rings are bridged by their nonbridging oxygen atoms (NBO's) via a Li bridge, their other NBO's being also terminated by lithium atoms. At this point it is useful to note that Uchino and Yoko[4] also find the eight-membered rings in their optimized structure; although they do not publish their calculated total energy, it appears that the highly symmetric structure found here should be more stable.

Structure I is closed as described above at this size of cluster; however, it is possible that it would be open in a much larger cluster, or in any case the closing of the chain would have a less significant effect on the total energy. Structures II and III (Figure 1ii,iii) are very similar, with a small variation in one of the terminal areas, and hence the small differences in the calculated bond lengths and vibrational spectra (see later). There also exists a significant similarity between II and III and the highly symmetric I; in particular we note again eight-membered metaphosphate rings, but then the NBO and Li bridging is more random. It is possible that structures such as II and III would exist in the bulk (i.e., not chain-ordered) part of a lithium phosphate glass with a 1:1 stoichiometry, given of course that small variations in the termination of the cluster model have been allowed for. Finally, structure IV, and other higher energy structures that are not given here, would represent more sparsely encountered areas of the material.

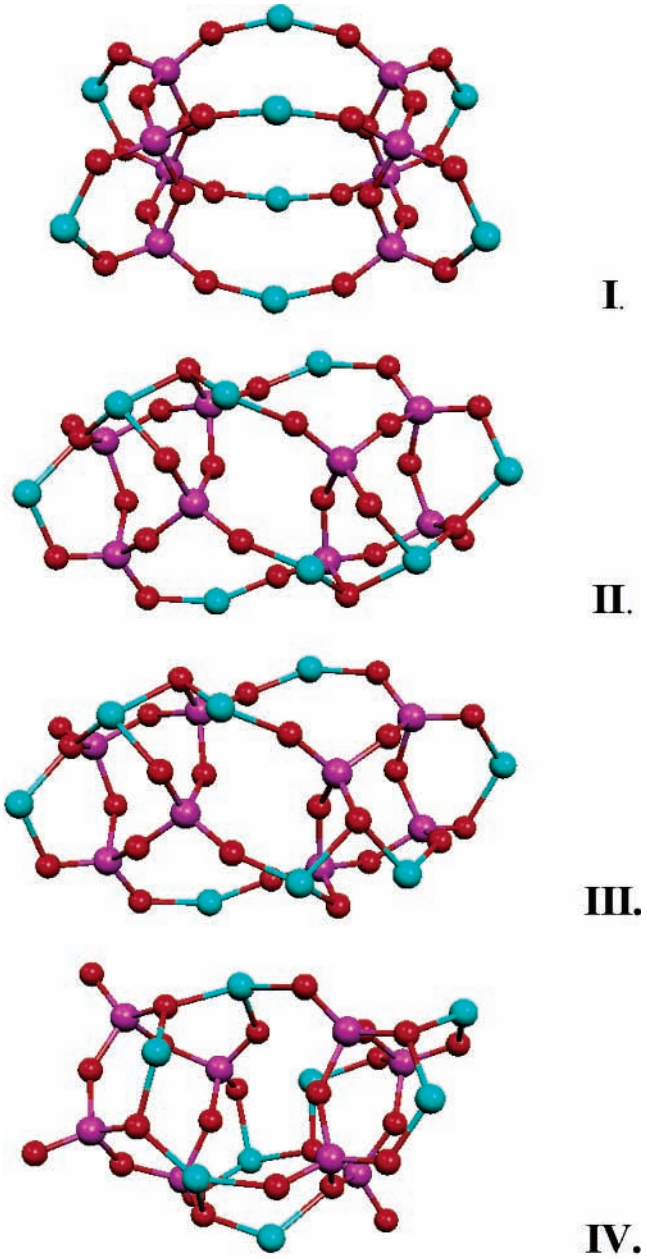

Figure 1. Structures I−IV calculated at the HF/3-21G* level: blue, Li; red, O; pink, P.

TABLE 1: Total Energy and Average Optimized $P-O_{nonbridging}$ and $P-O_{bridging}$ Bond Lengths for Structures I−IV

	energy (hartree)	$P-O_{nb}$ (Å)	$P-O_b$ (Å)	ΔE (kcal/mol)
I	−4561.507111	1.484	1.595	0
II	−4561.460653	1.499	1.597	29.1
III	−4561.453896	1.494	1.600	33.4
IV	−4561.447941	1.500	1.607	37.1

At this point it is useful to note that some, but not all, of the Li atoms in structures II and III appear in reasonable coordination numbers of 3 and 4. This may not be clear at first, but close examination shows that two Li atoms at the top left end and two more at the bottom right of II and III in Figure 1 have higher than two coordination numbers. This agrees well with ref 4 and shows that the constrained optimization in ref 4 and the unconstrained one performed here converge to a similar picture.

Overall we find structures that bear significant similarities, like the Li-bridged metaphosphate rings, but differ in energy. In a crystal, only the structure with the lowest energy would be favored; in a glass on the other hand, we suggest that the rapid cooling of the melt will give rise to more than one type of different local structure to be "trapped" in the material. These different local structures are modeled here by the multiple low-lying minima of the cluster model.

2. Vibrational Spectra. Full energy second derivatives and dipole moment derivatives were calculated for all four of the lowest-lying structures I−IV at the HF/3-21G* level of theory. First, the force constants calculation confirms that all structures represent minima of the potential energy surface. Second, we note that we will not follow the widely used practice to scale the HF/3-21G* frequencies by reducing them by a factor of 10%; Uchino and Yoko[4] use a factor of 0.93 to obtain the best possible agreement with experimental data. In this work, we will give all vibrational frequencies as calculated by the HF and DFT methods, without the introduction of scale factors, bearing in mind that the agreement with experiment might appear to be worse. It is, on the other hand, a true reflection of the capabilities of the theoretical methods, unaltered by empirical factors.

A complete list of the calculated harmonic vibrational frequencies and infrared intensities for all four structures at the HF/3-21G* level of theory is available upon request. In Table 2, the vibrational frequencies with a calculated infrared intensity above 90 km/mol for each of the four structures are given.

To facilitate the visualization of the great number of the calculated frequencies, especially in the lower symmetry structures II−IV, we represent each frequency by a Gaussian curve of the form $y = I_0 e^{-\ln 2(x-x_0/\sigma)^2}$, where x_0 is the position of the peak (in cm^{-1}) and the calculated integrated infrared intensity is given by $I_{calc} = I_0\sigma\sqrt{(\pi/\ln 2)}$. One of the two free parameters, half-width at half-height, σ, must be arbitrarily selected, so that the other parameter I_0, the height of the curve, is derived from the calculated integrated infrared intensity. Thus, the predicted infrared vibrational spectra that correspond to the four calculated structures I−IV are given in Figure 2, using a fixed width at half-height 2σ of 40 cm^{-1} for all peaks; this is arbitrary and serves only to provide a rough visual representation of the spectra.

We note in Figure 2 that there exists considerable resemblance between the four spectra; especially in the high-frequency part, due to the P−O stretches mainly, all spectra show peaks at approximately the same positions. This is also confirmed from the data of Table 2, where although in the cases of structures II−IV we see a significant splitting of the peaks of structure I that is more symmetric, the overall picture is similar. Things are quite different in the mid-frequency range, where peaks due to the vibrations of the whole framework of the clusters are differentiated between the four structures, even between II and III, which from Figure 1 can be seen to be very similar. Finally, the cation motion low-frequency area shows significant similarity between the four structures; this, in our view, can be

TABLE 2: Calculated Harmonic Vibrational Frequencies with a Predicted Integrated Intensity above 90 km/mol for All Four Lowest Lying Structures

I		II		III		IV	
ν (cm^{-1})	I (km/mol)	ν (cm^{-1})	I (km/mol)	ν (cm^{-1})	I (km/mol)	ν (cm^{-1})	I (km/mol)
142	93						
152	106						
293	96						
335	143						
348	92						
380	251						
		392	158	391	148	394	237
405	164						
				463	97	458	90
				471	166		
				477	94		
488	240	489	210	490	129		
		526	228	510	92		
		553	170			568	125
		579	212	550	99	576	185
						592	402
600	802			600	163	598	93
				604	209		
615	345	617	551			611	194
				621	141	626	244
		635	115	634	373	632	174
649	403			655	194		
		664	183			664	261
		668	220	668	160		
672	348	679	239	678	108	679	142
		690	405	685	265		
		695	207	688	211		
		708	371	704	121	711	258
				718	250	716	218
						723	186
						743	317
						763	282
						766	142
772	1229						
796	93	789	91	795	134	795	132
						798	305
816	111	817	127				
		823	256	820	173	819	108
		834	404	832	218		
				857	149		
				862	207		
900	471	896	213	900	265	907	232
926	482			925	156		
		1094	302	1094	205	1102	208
		1094	94	1116	376	1120	371
		1129	117	1133	326		
		1136	513	1136	690		
				1153	331	1160	519
						1165	670
						1168	255
						1173	254
1185	2699	1187	1465	1181	879		
		1191	1381	1187	215	1184	416
		1197	279	1197	592	1199	998
		1204	450	1208	581		
		1210	130	1210	975	1219	1300
		1232	292			1235	226
		1241	110			1243	188
						1249	302
1261	4644	1256	664	1262	750	1259	943
		1268	998	1279	487		
1310	90						
				1369	239		
		1374	187	1389	160	1391	978
		1387	468	1392	621	1398	377
				1412	747	1414	1041
1437	114	1432	2494	1431	1152		
1439	1179	1438	626	1439	967	1443	808
1447	4030	1445	407	1443	815		
		1491	610			1487	343
		1491	98	1492	335	1493	659
						1503	265

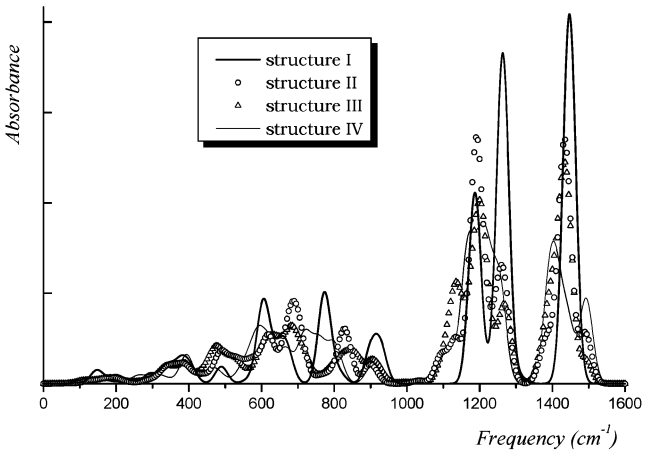

Figure 2. Predicted infrared spectra of I−IV visualized as described in the text.

TABLE 3: Predicted Vibrational Frequencies for All IR-Active Peaks and Their Intensities Calculated at the DFT Level of Theory for Structure I

ν (cm^{-1})	I (km/mol)	ν (cm^{-1})	I (km/mol)	ν (cm^{-1})	I (km/mol)
77	22	328	108	753	78
95	1	340	307	758	141
116	4	343	7	835	465
119	91	356	11	893	453
128	121	361	11	1069	2357
168	40	437	137	1127	1302
182	48	505	56	1173	223
199	7	541	913	1177	2703
200	28	542	57	1235	23
216	38	553	291	1361	174
237	55	580	5	1365	900
263	87	593	269	1372	3390
287	103	603	1		
309	25	693	122		
312	35	729	575		

attributed to the fact that the small Li cation sees in all cases a very similar "average environment"; this environment, however, may not be a very good representation of the true situation, as the fact that a limited model is used causes the average Li coordination to be smaller than in the material. It is noted that in the less than 380 cm^{-1} area structures II, III, and IV appear empty; for II and III the intense peaks at 335 and 348 cm^{-1} are split into many more with lower than 90 km/mol intensities, and there is an absence of intense peaks in the 140−150 cm^{-1} area. For IV we find a significant peak at 294 cm^{-1} with an intensity of 71 km/mol.

To obtain a better degree of accuracy we have reoptimized structure I at the density functional theory (DFT) level with the MPW1PW91 functional,[14] and also calculated the harmonic vibrational frequencies and IR intensities at this level. The calculated data are given in Table 3 (all IR active frequencies) and plotted in Figure 3 using the usual Gaussian function representation. A recent experimental IR spectrum[15] is also given in Figure 3. We adjust the half-widths σ used in the graph of theoretical data so that the experimental peaks are followed in the closest possible way.

A first observation is that there exists a shift, as expected, toward lower frequencies when going, for structure I, from HF (Figure 2 thick line) to DFT (Figure 3 thick line). It is also worth stressing the fact that although in Figure 2 the spectrum is plotted with a uniform "guessed" half-width at half-height of 20 cm^{-1}, in Figure 3 we try to represent the height of the

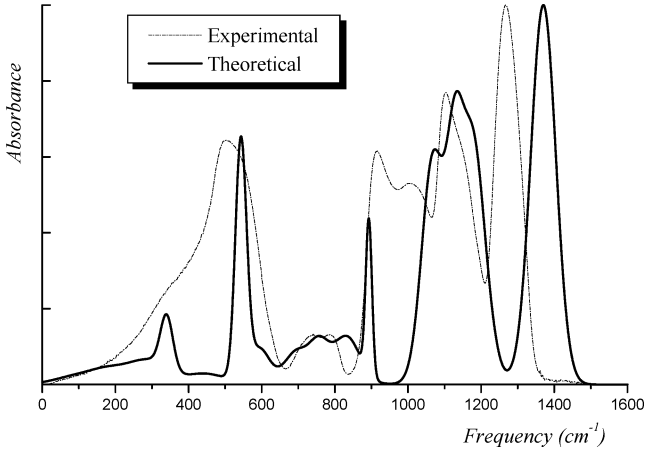

Figure 3. Calculated IR spectrum of structure I at the DFT level plotted as described in the text and the experimental IR spectrum of lithium metaphosphate.

TABLE 4: Calculated and Experimental Raman Spectra (Frequencies in cm^{-1}) for I

exp[16]	HF/3-21G*	DFT/3-21G*	symmetry
1260	1425	1352	b_{1g}
1160	1308	1228	a_g
670	796 631	725, 592	a_g, a_g
300	375, 366, 354, 341	338, 334, 323, 301	a_g, b_{2g}, b_{1g}, a_g

major peaks in the best possible way; this leads in some cases to much narrower peaks.

A very good overall agreement between the DFT predicted spectrum and the experiment is seen in Figure 3. Both the high-frequency peak and the low-frequency envelope are very well represented, and even the 600−800 cm^{-1} area shows a very good similarity between theory and experiment. The one notable difference is in the 900−1000 cm^{-1} relatively broad experimental peak, which does not seem to be well reproduced by theory; ring bending modes are present in this frequency range, and we attribute this discrepancy to the fact that the relatively small models used in the theoretical study cannot contain the entire range of various −O−P− rings present in the material.

The major DFT level predicted peaks of Figure 3 are described as follows

$$1372\ cm^{-1}\ b_{3u}\ P{-}O_{nb}\ \text{asymmetric stretch}$$

$$1177\ cm^{-1}\ b_{2u}\ P{-}O_{nb}\ \text{symmetric stretch}$$

$$1127\ cm^{-1}\ b_{2u}\ P{-}O_{b}\ \text{asymmetric stretch}$$

$$1069\ cm^{-1}\ b_{1u}\ P{-}O_{b}\ \text{symmetric stretch}$$

$$893\ cm^{-1}\ b_{3u}\ \text{bridging Li motion}$$

$$541\ cm^{-1}\ b_{2u}\ \text{skeletal bend}$$

$$340\ cm^{-1}\ b_{2u}\ P{-}O{-}Li{-}O{-}P\ \text{bend}$$

Finally, Table 4 summarizes the most intense Raman active peaks as predicted at the HF and DFT levels of theory. Excellent agreement, given a uniform shift that is smaller in the DFT case, is found with the experimental spectrum.[16]

Conclusions

In this work, we present a detailed approach of the study of the structure and vibrational spectrum of a glass system by

molecular electronic structure theory methods. An approach that involves using both semiempirical and ab initio or density functional theory methods is presented; using these two approaches in parallel, we map a large portion of the potential energy surface of a relatively large cluster model of the material, in this way finding multiple low-lying minima.

The lithium metaphosphate glass $(Li_2O{\cdot}P_2O_5)_n$ is studied as a first example, where for $n = 4$, we find the four lowest lying structures of the potential energy surface of the model. The energetics and structural parameters of these structures, which could represent models for the local structure of the glass, are given, although it is not attempted at this stage to calculate statistical distributions based on the calculated energies. Among other reasons for this, the most important one would be that a small cluster such as the one studied here would be abnormally stabilized energetically by, for example, the ring closure found in structure I due to its small size, which would not be as important in a continuous chain structure of the solid.

The predicted vibrational spectra are presented in detail, both in numerical and in graphical form. Findings can be summarized as follows:

(a) All structures calculated show clearly the types of modes expected in the frequency ranges expected and are in good agreement with experiment . Similarity between the spectra of Figure 2 suggests that all structures could be present in the macroscopic material. However, greater accuracy in the calculation is needed, possibly at the DFT level, so that a *weighted* summation of the spectra from the different structures will provide clearer insight into the structure of the amorphous material.

(b) A DFT spectrum of the lowest energy structure I shows very good agreement with an experimental IR spectrum of the lithium metaphosphate glass. It is hence clearly shown by this theoretical investigation that, as proposed in the past by experimental studies, the glass is dominated by Li-bridged $PO_2O_{2/2}$ chains

Acknowledgment. We thank Drs. C. Varsamis and E. I. Kamitsos for communicating to us the experimental spectrum of lithium metaphosphate glass, and also for many discussions on the subject.

References and Notes

(1) Liang, J.-J.; Cygan, R. T.; Alam, T. M. *J. Non-Cryst. Solids* **2000**, *263 & 264*, 167.
(2) O'Keeffe, M.; Domenges, B.; Gibbs, G. V. *J. Phys. Chem*. **1985**, *89*, 2304.
(3) Uchino, T.; Ogata, Y. *J. Non-Cryst. Solids* **1995**, *181*, 175.
(4) Uchino, T.; Yoko, T. *J. Non-Cryst. Solids* **2000**, *263 & 264*, 180.
(5) Wright, A. C.; Hulme, R. A.; Grimley, D. I.; Sinclair, R. N.; Martin, S. W.; Price, D. L.; Galeener, F. L. *J. Non-Cryst. Solids* **1991**, *129*, 213.
(6) Hudgens, J. J.; Brow, R. K.; Tallant, D. R.; Martin, S. W. *J. Non-Cryst. Solids* **1998**, *223*, 21.
(7) Dewar, M. J. S.; Reynolds, C. H. *J. Comput. Chem*. **1986**, *2*, 140.
(8) Stewart, J. J. P. *J. Comput. Chem*. **1989**, *10*, 209.
(9) Stewart, J. J. P. *J. Comput. Chem*. **1989**, *10*, 221.
(10) Binkley, J. S.; Pople, J. A.; Hehre, W. J. *J. Am. Chem. Soc*. **1980**, *102*, 939.
(11) Petersson, G. A.; Benett, A.; Tensfeldt, T. G.; Al-Laham, M. A.; Shirley, W. A.; Mantzaris, J. *J. Chem. Phys*. **1988**, *89*, 2193.
(12) Frisch, M. J;. et al. *Gaussian 98*, revision A.9; Gaussian: Pittsburgh, PA, 1998.
(13) Hudgens, J. J.; Martin, S. W. *J. Am. Ceram. Soc*. **1993**, *76* (7), 1691.
(14) Adamo, C.; Barone, V. *Chem. Phys. Lett*. **1977**, *271*, 242.
(15) Varsamis C. Private communication.
(16) Rouse, G. B.; Miller, P. J.;. Risen, W. M., Jr. *J. Non-Cryst. Solids* **1978**, *28*, 193.